

INVESTIGATION OF THE BEHAVIOUR IN CHLORIDE SOLUTION OF ALUMINIUM ALLOYS AS MATERIALS FOR PROTECTOR PROTECTIONS

RAZISKAVA VEDENJA ALUMINIJEVE ZLITINE, MATERIALA ZA VAROVALNE ELEKTRODE, V KLORIDNI RAZTOPINI

Darko Vuksanović¹, Petar Živković¹, Dragan Radonjić¹, Branka Jordović²

¹University of Montenegro, Faculty of Metallurgy and Technology, Cetinjski put bb, 81000 Podgorica, Republic of Montenegro

²Technical Faculty of Čačak, Svetog Save 65, 32000 Čačak, Republic of Serbia

darkov@cg.ac.yu

Prejem rokopisa – received: 2007-02-02; sprejem za objavo – accepted for publication: 2008-02-05

The aim of the investigations was to check the behaviour of Al-Zn-Sn aluminium cast alloys with additions of bismuth and gallium for potential application as a material for protecting protectors. The chemical composition, the mechanical characteristics, the microstructure and the corrosion properties were investigated. Particular attention was given to microstructural investigations aimed to identify the phases that might have an active role for corrosion in chloride solution. Three corrosion tests were used: change in the corrosion potential with time, determination of the values for polarisation resistance and the corrosion current, and potentiodynamic recording of the cathode and anode polarisation curves.

Key words: aluminium alloys, chloride solution, corrosion potential, polarisation resistance, corrosion current, polarisation curves

Cilj raziskave je bil preveriti vedenje litih zlitin Al-Zn-Sn z dodatkom bismuta in galija kot možnih materialov za varovalne elektrode. Kemijske sestava, mehanske lastnosti, mikrostruktura in korozjske značilnosti so bile opredeljene. Posebna pozornost je bila namenjena mikrostrukturnim preiskavam, da se določi, katere faze bi lahko imele aktivno vlogo pri koroziji v kloridni raztopini. Ugotovljeno so bile tri korozjske značilnosti: sprememba korozjskega potenciala s časom, polarizacijska upornost in gostota toka ter potenciodinamični katodna in anodna polarizacija.

Ključne besede: aluminijeve zlitine, kloridna raztopina, koroziski potencial, polarizacijska upornost, koroziski tok, polarizacijske krivulje

1 INTRODUCTION

The corrosion damage of various constructions, such as machines, vessels pipelines, ships, oil pipelines, docks is effectively resolved with electrochemical (i.e., active) protection. One of the procedures used is the protection of protectors that are applied for infrastructural objects, e.g., warehouses, shipyards, heat exchangers, and machines operating in aggressive environments, especially in the presence of chlorides. The procedure is based on the use of more electronegative alloys as the protectors (galvanic anodes or sacrificial anodes). The results of these investigations demonstrate the importance of using the proper method for the preparation of aluminium alloys.

Several factors influence the investigated protector alloys – the chemical composition, the alloying procedure the casting and the thermal treatment – and only with proper processing a high-quality alloy will be obtained.

2 EXPERIMENTAL

The protector alloys were melted in an electroresistive furnace using a graphite crucible. The experi-

mental work consisted of four parts: 1) the preparation of alloys; 2) chemical analysis, determination of the mechanical properties and of the microstructure; 3) determination of the corrosive and electrochemical characteristics of alloys in a solution of 0.51 M of NaCl; 4) examination of the microstructure before and after the corrosion test. The chemical analysis was performed with an X-ray quantometer; the tensile strength, the yield point ($R_{0.2}$) and the relative elongation were determined with an electronic, universal tensile-testing machine in the company Kombinat Aluminium Podgorica. The corrosion tests were performed on computerised equipment using a saturated calomel electrode as a reference, while the metallographic analysis and the electron-probe microanalysis was carried out at the Technical Faculty of Čačak. For the qualitative metallographic analysis, the method of area assessing for the intermetallic phases, and linear intercept of the width of the secondary dendrite arms of the Al solid solution (DAS) were used. The DAS parameters were determined to verify the eventual influence of added elements on the hardening process and on the behaviour of the alloy in an aggressive environment. A scanning electron microscope (SEM) was used for the energy-dispersive x-ray spectroscopy (EDS).

3 RESULTS AND DISCUSSION

The chemical composition of the alloys is shown in **Table I**, and in **Table II** the mechanical properties of the cast alloys are presented. The content of zinc was in range 3.90–4.90 %, that of tin (with the exception of

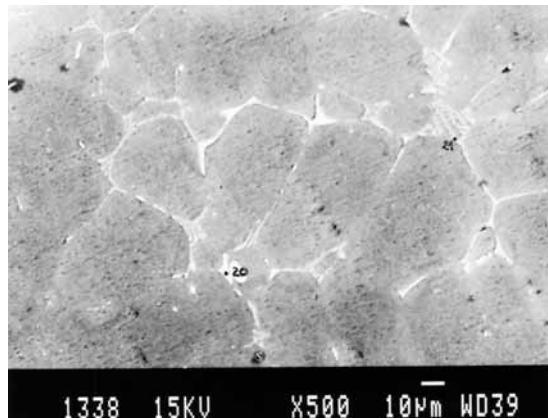


Figure 1: Microstructure of alloy 1 before the corrosion test. Magn. 500-times

Slika 1: Mikrostruktura zlitine 1 pred preizkusom korozije. Pov. 500-kratna

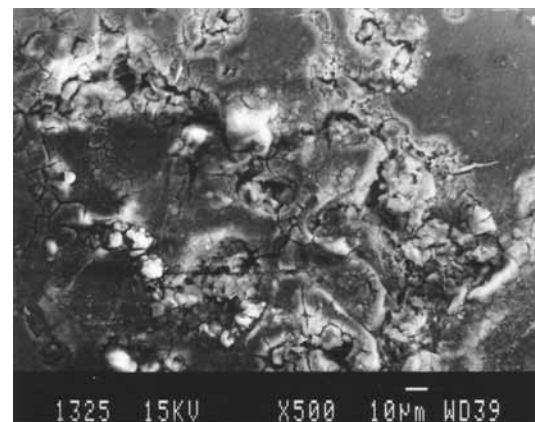


Figure 2: Microstructure of the alloy 1 after the corrosion test in 0.51-M NaCl. Magn. 500-times

Slika 2: Mikrostruktura zlitine 1 po preizkusu korozije v 0.51 M NaCl. Pov. 500-kratna

alloy 2) was 0.16–0.64 %, the content of bismuth in alloys 1 and 2 was 0.2–0.3 %, and that of gallium was 0.5 % in all alloys. The amounts of iron, silicon, titanium and copper were similar in all alloys.

The as-cast alloys have a low tensile strength and hardness, and a relatively large elongation. This combination of properties is favourable from the aspect of

Table I: Chemical composition of the alloys in mass fractions (w/%)

Tabela I: Kemična sestava zlitin v masnih deležih (w/%)

Alloy	Al	Zn	Sn	Bi	Ga	Fe	Si	Ti	Cu	V
1	94.209	3.9	0.64	0.2	0.5	0.36	0.11	0.012	0.05	0.01
2	94.794	3.95	-	0.3	0.5	0.28	0.11	0.008	0.04	0.01
3	94.035	4.9	0.16	-	0.5	0.27	0.1	0.007	0.01	0.01
4	94.613	3.95	0.47	-	0.5	0.28	0.1	0.009	0.06	0.01

Table II: Mechanical properties of the as-cast alloys

Tabela II: Mehanske lastnosti litih zlitin

Alloy	$R_{0.2}$ / (N/mm ²)			R_m / (N/mm ²)			A/%			HB / (N/mm ²)		
	1	44.5	69.7	6.8	30.3							
2		45.6	52.2	4.0	34.6							
3		47.5	97.1	14.4	30.9							
4		43.5	67.5	5.6	31.9							

Table III: Quantitative indicators for the microstructure of as-cast alloys

Tabela III: Kvantitativni kazaleci za mikrostrukturo litih zlitin

Alloy	Surface of particle, IMF, $A/\mu\text{m}^2$			Perimeter, $L_p/\mu\text{m}$			Shape factor of perimeter			Shape factor of surface			Dendrite arm spacing $DAS/\mu\text{m}$			V_v , % $\text{Na}\cdot 10^3$ μm^3 *		
	min	max	sr	min	max	sr	min	max	sr	min	max	sr	min	max	sr			
1	Al ₃ Fe	0.12	35	2.9	1.4	83	10	0.04	0.94	0.47	0.09	1	0.84	5.9	165	44	0.6	2.1
	SnBiAl	0.66	74	7.0	3.3	51.6	12	0.11	0.98	0.65	0.56	1	0.94				0.4	0.6
2	Al ₃ Fe	0.08	5.8	0.6	1.1	22.7	3.6	0.08	0.93	0.61	0.2	1	0.91	6	138	43	0.4	5.6
	BiZnAl	0.5	14.2	3.2	2.6	14.2	6.1	0.6	0.97	0.89	0.9	1	0.98				0.11	0.4
3	Al ₃ Fe	0.08	23.7	2.4	1.2	51	8.7	0.06	0.96	0.47	0.14	1	0.85	6.9	155	48	0.5	1.99
	SnAl	1	25	5.7	3.9	31	9.7	0.2	0.98	0.77	0.4	1	0.96				0.2	0.34
4	Al ₃ Fe	0.1	29	2.9	1.5	71	11	0.04	0.95	0.43	0.1	1	0.8	9.7	160	46	0.6	2.17
	SnAl	0.9	20	5.5	3.7	42	10	0.1	0.98	0.75	0.3	1	0.95				0.4	0.77

*Numerical density

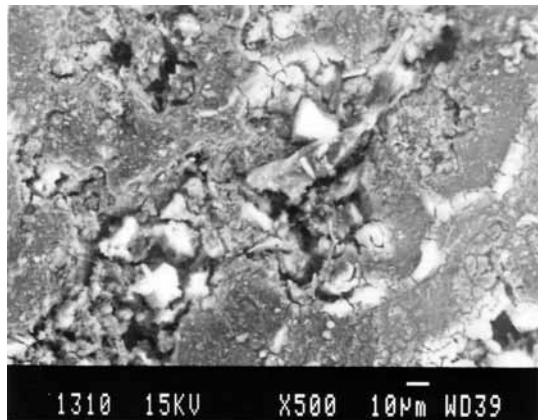


Figure 3: Microstructure of alloy 1 after the corrosion test in 0.051-M NaCl. Magn. 500-times

Slika 3: Mikrostruktura zlitine 1 po preizkušu korozije v 0.051 M NaCl. Pov. 500-kratna

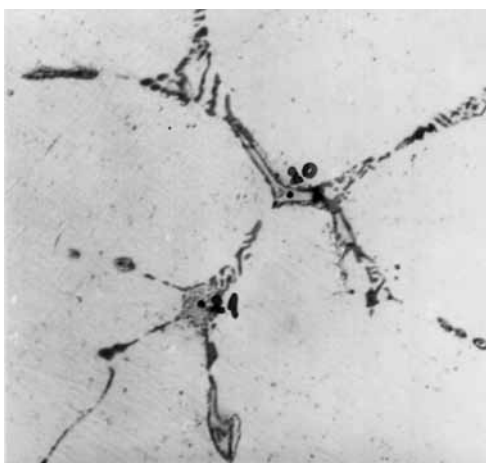


Figure 4: Microstructure of the alloy 1, phases Al_3Fe and SnBiAl . Magn. 730-times

Slika 4: Mikrostruktura zlitine 1, fazi Al_3Fe in SnBiAl . Pov. 730-kratna

the alloys' application, because their static and dynamic loading does not require a particular strength.

A detailed examination of the microstructure was carried out only for alloy 1, which contains all the elements of interest and relevant for the protection suitability. In **Table III** the quantitative indicators for the constituents of the microstructure of the cast alloys are shown, while the microstructure of alloy 1, before and after the corrosion test, is shown in **Figures 1 to 4**.

The alloys have a multiphase microstructure consisting of an Al solid solution and several phases, which differ in shape, size and distribution across the section of the sample. The phases AlBiSn and Al_3Fe were found in alloy 1. Phases based on gallium were not found, probably because of the unsuitability of the analytical equipment. From microstructural observations it was concluded that the gallium phases are located at the grain boundaries as well as inside the cells and dendrites.

In all the alloys an intermetallic phase based on aluminium and iron, with a small amount of zinc and silicon was found. According to the intensity of the

peaks on the recorded spectra and the particles morphology, the light-grey Al_3Fe phase that also contains zinc and silicon (**Figure 5**). As shown in the micrographs (**Figures 1 and 4**, mark 21), this phase is the eutectic constituent formed at the end of solidification. The particles of this phase are mainly in the shape of platelets of different size (**Table III**), when they are found in the normal degenerated eutectic. The volume share of this phase is in range 0.4–0.6 %. The total volume share of the intermetallic phases in all the investigated alloys was in the range 0.5–1.0 %. The type of second intermetallic phase depends on the chemical composition of the alloy. In alloy 1 the AlBiSn (**Figures 1 and 4**, mark 20) phase is present in the form of coarse, isolated particles with different shapes (angular, round, plate), and its composition is confirmed by the high intensity of the tin peak in **Figure 6**. Particles of this phase are found mostly at the dendrite boundaries. This phase remains bright after etching, since it is not attacked by the Keller's reagent. Its content (**Table III**) is particularly high in alloy 1, with the highest content of tin.

In alloy 2 the distribution of the phase Al_3Fe is very uniform (**Table III**). In addition to this phase the analysis showed a small amount of the AlBiZn phase (0.11 %) (**Figure 7**), mostly in the form of rounded

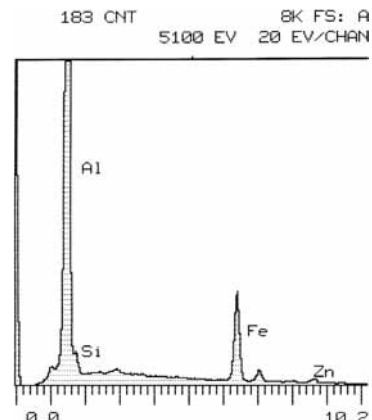


Figure 5: Maximum peak intensities, phase Al_3Fe
Slika 5: Največe intenzitete, faza Al_3Fe

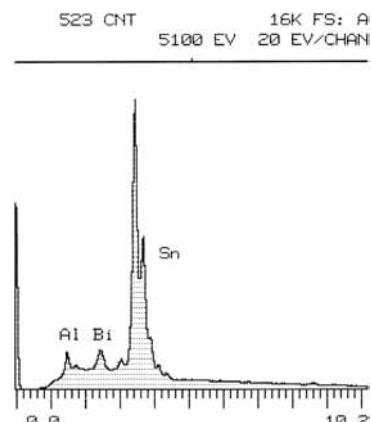


Figure 6: Maximum peak intensities, phase AlBiSn
Slika 6: Največe intenzitete, faza AlBiSn

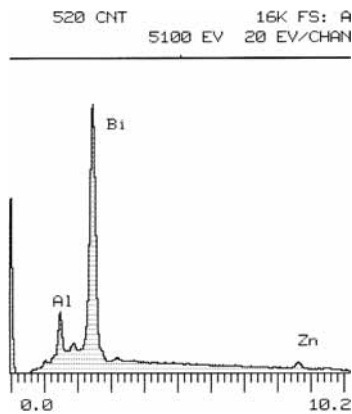


Figure 7: Maximum peak intensities, phase AlBiZn
Slika 7: Najveće intenzitete, faza AlBiZn

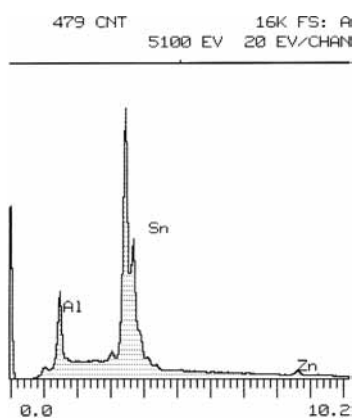


Figure 8: Maximum peak intensities, phase AlSn
Slika 8: Najveće intenzitete, faza AlSn

particles at the boundaries; however, it is also inside the dendrites. A characteristic of this alloy are the small amounts of intermetallic phases (in total 0.5 %), which can probably be attributed to the absence of tin, which can form several intermetallic phases in these types of alloys. The analysis shows (**Table III**) that in alloys 3 and 4 a small amount of zinc is present in the phase AlSn (**Figure 8**).

The microstructural observations after a treatment in the chloride solution show the strongest attack taking place at the cellular-dendrite boundaries, where the intermetallic phases with a different electrochemical potential are located. During the corrosion test more of the matrix was dissolved than of the AlSn and AlBiSn phases. Also, the phases AlBiSn, AlBiZn and AlSn were dissolved during the test in the 0.51 M NaCl solution.

In **Tables IV and V** the values of the corrosion characteristics of the alloys in the 0.51 M NaCl solution are shown, while in **Figures 9 to 12** the recordings on the tests of alloy 1 are shown. The analysis of the corrosion potential vs. time in 0.51 M NaCl indicates the temporal evolution of the potential to more positive values, up to the final value of -1327 mV. The negative value of the final potential is explained by the rapid dissolution in the test solution and by the rapid increase in the concentration of ions in the vicinity of the

electrode (**Figure 11**) and the slow diffusion of ions from the electrode area. At a corrosion potential of -1327 mV, in the 0.51 M NaCl solution the polarisation resistance and the corrosion current are $R_p = 0.1266 \text{ k}\Omega$ and $j_{corr} = 171.43 \mu\text{A}/\text{cm}^2$ (**Figure 12**).

During the test in the 0.51 M NaCl solution the dissolution of the alloy occurred virtually only at the grain boundaries where the AlBiSn particles were present. This could explain, for alloy 1, the very negative corrosion potential, the lower polarisation resistance and the higher corrosion currents. From the corrosion characteristics in Tables IV and V we can conclude that for a test in a more concentrated solution, such as the NaCl solution, a larger extent of solution of the phases provides a good characterization of the investigated alloy in terms of the application for protectors' protection.

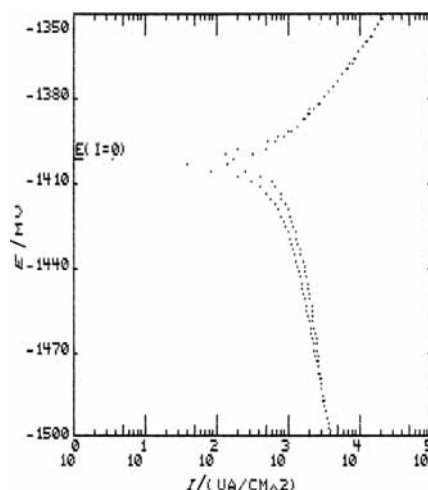


Figure 9: Potentiodynamic cathodic and anodic polarization curves for alloy 1 in 0.51 M NaCl. Scan rate 1 mV/s
Slika 9: Potenciodinamični katodna in anodna polarizacijski krivulji za zlitino 1 v 0.51 M NaCl. Hitrost skaniranja 1 mV/s

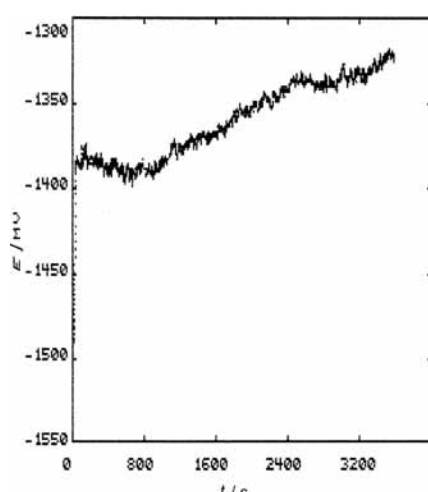


Figure 10: Corrosion potential vs. time for alloy 1 in 0.51 M NaCl
Slika 10: Časovna odvisnost koroziskskega potenciala za zlitino 1 v 0.51 M NaCl

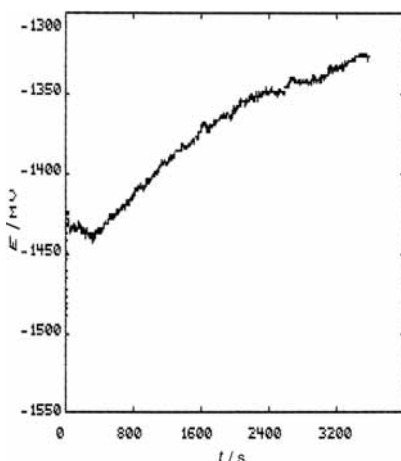


Figure 11: Corrosion potential vs. time for alloy 1 in 0.51 M NaCl
Slika 11: Časovna odvisnost korozijskega potenciala za zlitino 1 v 0.51 M NaCl

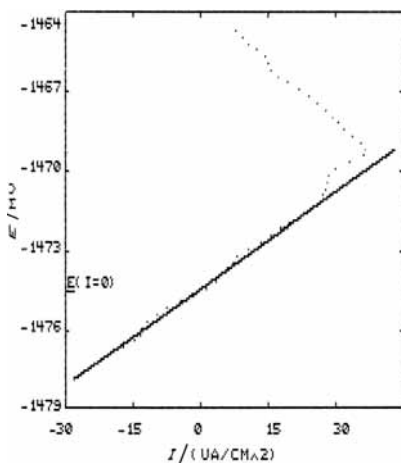


Figure 12: Polarization resistance for alloy 1 in 0.51 M NaCl. Scan rate 1 mV/s
Slika 12: Polarizacijska upornost za zlitino 1 v 0.51 M NaCl. Hitrost skaniranja 1 mV/s

Table IV: Dependence of corrosion potential vs. time in 0.51 M NaCl
Tabela IV: Odvisnost korozijski potencial – čas v 0.51 M NaCl

Alloy	$E_{\text{begin}}/\text{mV}$	E_{end}/mV
1	-1491	-1327
2	-1380	-1324
3	-1376	-1330
4	-1406	-1336

Table V: Polarization resistance in 0.51 M NaCl
Tabela V: Polarizacijska upornost v 0.51 M NaCl

Alloy	$E_{\text{corr}}/\text{mV}$	$E(j=0)/\text{mV}$	$R_p/\text{kΩ}$	$j_{\text{corr}}/(\mu\text{A}/\text{cm}^2)$
1	-1469.25	-1474.75	0.1266	171.43
2	-1355.166	-1362.25	0.1936	112.12
3	-1334.2	-1345	0.0953	227.8
4	-1361.5	-1375	0.2065	105.14

During the corrosion test for the AlBiSn and AlBiZn phases, higher values of polarisation resistance and lower corrosion currents were obtained than for the phase AlSn in alloy 3. In the presence of the phase AlSn, alloy 4 shows a lower corrosion current and a higher polarization resistance than alloy 3, although the tin content is higher in alloy 4. The difference may be related to the difference in the content of zinc, which is lower in alloy 4.

4 CONCLUSION

The experimental findings in this investigation show that:

- the investigated alloys have poor mechanical characteristics and cannot be used in cases of significant static and dynamic stressing;
- the chemical composition strongly affects the corrosion activity of the aluminium alloys;
- the solution of the matrix is faster at the grain boundaries than the solution of the AlSn and AlSnBi phases;
- the alloys 3 and 4 show great corrosion activity in chloride solutions, while alloy 3 shows better corrosion characteristics.

It is justifiable to continue with the investigations on alloy 3 with the aim to verify the effect of the content of tin on the corrosion activity.

5 REFERENCES

- ¹ L. F. Mondolfo, Aluminum alloys-structure and properties, Butterworths, 1976
- ² S. A. Ginzberg, Formation and dissolution behavior of anodic oxide films on aluminum, Japan 1979, 438–456
- ³ J. G. Ivašina, L. E. Šprengelj, Zaštita truboprovodov ot korozii, 1980, 5–7
- ⁴ D. R. Salinas, S. G. Garcia, J. B. Bessone, Influence of alloying elements and microstructure on aluminium sacrificial anode performance: case of Al-Zn, Journal of Applied Electrochemistry, 29 (1999) 9, 1063–1071
- ⁵ S. Valdez, M. A. Talavera, J. Genesca, J. A. Juarez-Islas, Activation of an Al-Zn-Mg-Li alloy by the presence of precipitates to be used as sacrificial anode, Mat. Res. Soc. Symp. Proc., 654 (2001), 351–356